THE ASTROPHYSICAL JOURNAL, 240:612–618, 1980 September 1

A LOWER LIMIT ON THE MAGNITUDE OF THE COMPANION TO HDE 226868 (CYGNUS X-1)

ALLEN W. SHAFTER,[1] RICHARD J. HARMS,[2] BRUCE MARGON,[1,3] AND JONATHAN I. KATZ[1,3,4]
University of California
Received 1980 January 21; accepted 1980 March 6

ABSTRACT

High-precision digital spectra of the HDE 226868/Cygnus X-1 system have been obtained at a variety of orbital phases, using a Digicon photon counting array at the coudé focus of the Lick Shane reflector. The spectra have been cross-correlated to search for evidence for the existence of a luminous stellar companion to HDE 226868, as has been suggested by several models where the secondary star is not a black hole. We find no evidence for such a star and place a lower limit on the difference between HDE 226868 and its companion of 4 magnitudes. This limit rules out all of the models for the Cygnus X-1 system calculated by Avni and Bahcall which include main-sequence stars as secondaries rather than black holes. A merit function generally useful for cross-correlation of digital spectra is described.

Subject headings: stars: individual — X-rays: binaries

I. INTRODUCTION AND OBSERVATIONS

Cygnus X-1, the companion of the single-lined spectroscopic binary HDE 226868, is often cited as a strong candidate for a black hole. The spectroscopic and photometric data imply that the mass of the as-yet-unseen secondary star in the system is $\sim 14\ M_\odot$ (Bolton 1972; Hutchings *et al.* 1973; Hutchings 1974). The luminous, rapidly variable X-ray source points toward the presence of a compact object in the system. If the X-ray source *is* compact, and if this compact star and the massive secondary are in fact the same object, the implied mass exceeds that normally attributed to white dwarfs and neutron stars, arguing therefore for a black hole. There is no direct observational proof of these last hypotheses, however. For example, the X-ray emission may instead be produced in a small volume on a nondegenerate star (Bahcall, Rosenbluth, and Kulsrud 1973), perhaps thus explaining the uniquely different temporal behavior of the X-ray intensity compared with the accretion-powered binary X-ray systems. Alternatively, the X-ray source could be a neutron star, as is thought to be the case in the majority of the other luminous galactic X-ray sources, in a triple system which also includes the observed O9 supergiant and a much lower-luminosity, early type normal star (Fabian, Pringle, and Whelan 1974; Bahcall *et al.* 1974). Although the evolutionary history of such a system might be obscure (Shipman 1975), in at least one sense this model is less ad hoc than the black hole hypothesis, since many neutron star X-ray sources and numerous triple systems are known to exist, while there is little independent evidence for a black hole.

All of the above alternatives to a black hole in Cyg X-1 share in common the prediction that the massive unseen secondary of HDE 226868 is a relatively normal, luminous star. However, such an object would be very difficult to detect as a result of its low contrast against the extremely luminous supergiant companion. An attempt to test the three-body model via a search for perturbations on the binary velocity curve (Abt, Hintzen, and Levy 1977) has been inconclusive, because of the very small expected perturbation amplitude. It has been claimed that existing observations can "severely restrict or disprove" the presence of an ordinary star of the inferred mass of the secondary (Bolton 1975*a*). Avni and Bahcall (1975), however, have concluded that, consistent with all of the available data, the mass of the secondary could be as low as 8–9 $M_\odot$. In this case, the existence of a luminous secondary cannot be ruled out by present observations, although such an object might be detectable with very accurate ($\sim 1\%$) high-resolution spectrophotometry (Avni and Bahcall 1975).

In this paper we describe new observations, and a new technique for their analysis, which significantly constrain possible luminous secondary stars in the Cyg X-1/HDE 226868 system. Our technique of analysis should also be applicable to other single-lined spectroscopic binaries.

The data described here we obtained in 1977 June at the coudé focus of the Lick Observatory 3 m Shane reflector, using a 212 element Digicon array (Beaver and McIlwain 1971; Beaver, Harms, and Schmidt 1976) as a detector. On most nights observations were made at three different central wavelengths, covering a variety of different absorption features at different

[1] Department of Astronomy, Los Angeles.
[2] Department of Physics, San Diego.
[3] Alfred P. Sloan Foundation Research Fellow.
[4] Institute of Geophysics and Planetary Physics, Los Angeles.

TABLE 1

JOURNAL OF OBSERVATIONS

Principal Absorption Feature	Dispersion (Å per diode)	Coverage (Å)	Julian Date (2,440,000+)	ϕ[a]
λ4026 He I	0.17	34	3319.833	0.90
			3320.802	0.07
			3320.979	0.10
			3321.875	0.26
λ4471 He I	0.41	82	3320.927	0.09
			3321.948	0.28
			3322.917	0.45
λ5876 He I	0.25	51	3320.865	0.08
			3321.792	0.25
			3322.802	0.43
			3323.833	0.61

[a] Orbital phase using Bolton's 1975*a* convention and elements.

orbital phases spanning almost an entire 5.6 day orbital period. A journal of observations giving details of the individual spectra is given in Table 1, and the data are displayed in Figure 1. To avoid problems of aliasing, the data are oversampled, yielding 816 data points in each spectrum. Typical exposure times (through thin cloud) of 1.5–2 hr yielded at least 10^4 counts per channel in each spectrum, and features of a few percent of the continuum strength are easily visible in the figure. The spectra have been divided by the spectrum of a continuous lamp obtained just before or after the stellar spectrum, to remove channel-to-channel detector irregularities.

II. THE MERIT FUNCTION

In order to cross-correlate the spectra, we compute a merit function, $Q(K)$,

$$Q(K) = \int \prod_i S_i(\lambda - \Delta\lambda_i[\lambda, K])d\lambda ,$$

where $S_i = i$th spectrum, and $\Delta\lambda_i(\lambda, K)$ = wavelength shift of rest wavelength λ at the time of ith spectrum for an orbit with elements K.

The calculation of $Q(K)$ consists of shifting the spectral arrays with respect to each other by an amount $\Delta\lambda_i$ which corrects for the orbital Doppler shift, multiplying the fluxes at all epochs and summing. Then, if the hypothetical orbital elements K agree with the actual elements of either the primary or secondary, the spectral features will align and $Q(K)$ will reach a maximum. K may, in principle, denote the full set of orbital elements, but in practice we have used only the velocity semiamplitude; the period, phase, and eccentricity have been taken from published analysis of the primary spectrum (Bolton 1975*a*).

Using K as a free parameter, the plot of $Q(K)$ can be constructed. The shape of the resulting $Q(K)$ curve will depend on several factors. In the case of a single-line spectroscopic binary, $Q(K)$ will have a maximum at the semiamplitude of the visible component. The width of this maximum will be sensitive to the velocity width of the spectral lines being correlated and to the orbital phases of the spectra. Spectra taken at orbital phases when the star has high radial velocity will have $\Delta\lambda_i(K, \lambda)$ which is more sensitive to a change in K than $\Delta\lambda_i(K, \lambda)$ for spectra at other phases. As a result, the sensitivity of Q and K depends on how the observations are distributed around the orbit.

For a double-lined spectroscopic binary, the shape of $Q(K)$ becomes more complex. In addition to the factors mentioned for the single-line system, the relative velocity and intensities of the two components become important. For a double-line system, $Q(K)$ may have two separate maxima (corresponding to the primary and secondary), or one asymmetric maximum, depending on the wavelength separation of the primary and secondary line profiles in the spectra. Since this depends on the orbital phases of the data, the shape of $Q(K)$ depends critically on when the data were taken. If the primary and secondary lines are well separated, then $Q(K)$ should have separate maxima. However, if the secondary line profile occurs in the wing of the primary line, then $Q(K)$ will have a single asymmetric maximum. The He I profiles we consider may be time-variably asymmetric because of a wind from HDE 226868. However, this asymmetry is probably not a function of orbital phase and, consequently, is unlikely to confuse $Q(K)$ by mimicking the effect of a secondary.

If interstellar absorption lines are present, as is the case with HDE 226868, they may confuse $Q(K)$ by adding a separate peak at $K \approx 0$ or by causing an asymmetry in the primary peak. The actual effect will depend on the strength and width of the interstellar lines, the width of the primary peak, and the semiamplitude of the more massive component.

The potential advantage of a merit function like our $Q(K)$ is that it can combine information spread over many spectral lines, or many separate spectra, and

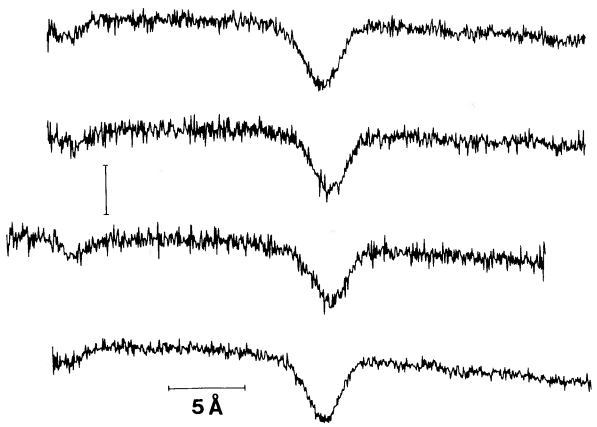

FIG. 1a

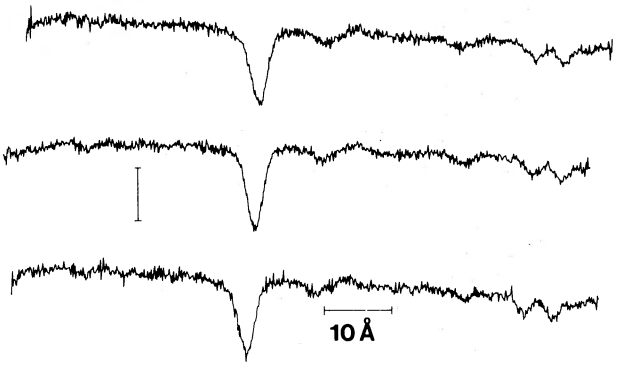

FIG. 1b

FIG. 1.—Spectra of HDE 226868 obtained with the Digicon at the coudé focus of the Lick Observatory 3 m Shane reflector. The details of each spectrum are given in Table 1, and the spectra are displayed in chronological order, earliest spectrum on top. The data are aligned in wavelength, and the orbital Doppler shift of the primary is readily apparent. The vertical bar on each panel represents 20% of the mean continuum intensity. (*a*) Spectra centered near He I 4026; (*b*) spectra centered near He I 4471; (*c*) spectra centered near He I 5876; note also the prominent interstellar Na D absorption lines.

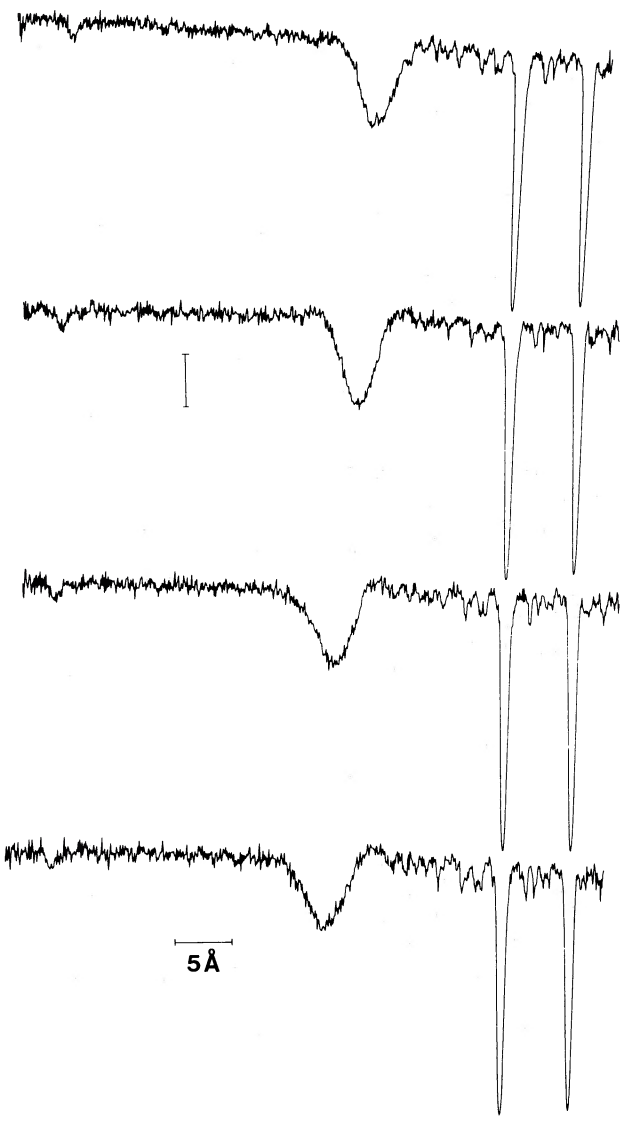

FIG. 1c

correlate scraps of information which are individually lost beneath noise and confusion. Unfortunately, when there are only a few strong lines, as in our spectra, the occasional accidental Doppler shift of one line to the rest wavelength of another introduces large spurious signals into $Q(K)$. We expect use of this function to be more fruitful for spectra with many lines, in which case averaging of many spurious signals reduces them to a mean noise background.

III. ANALYSIS

Before the spectra of the Cyg X-1/HDE 226868 system could be correlated, it was necessary to remove any low-frequency trends in the data. If left in, the trends would drown any real signal in $Q(K)$ in a spurious background trend. The low-frequency filtering was accomplished by fitting a third-order polynomial to the continuum of each spectrum and then subtracting the resulting polynomial from the data. A constant was then added to the filtered data to restore the continuum to approximately its original intensity. The choice of the additive constant affects the height of the peak in $Q(K)$, compared to its mean level, but empirically was found to have little effect on its sensitivity to the presence of a secondary.

The observed spectra contain other lines in addition to the principal absorption features, some of which are closely spaced (e.g., interstellar Na D lines in the λ5876 spectra and stellar nitrogen lines in the λ4471 spectra). In order to avoid accidental correlations between neighboring features, which for our spectra were found to confuse $Q(K)$, we only include in our computations a narrow region centered on the principal absorption feature and excluding these sources of spurious correlations. Sufficient data were correlated on both sides of the primary feature to include the

secondary feature out to any reasonable $|K|$ (400 km s^{-1}) and its wings. In addition, for the second set of spectra, a sufficient bandwidth was correlated to include the Mg II 4481 feature, as well as the stronger He I 4471.

If a luminous secondary is present, the secondary line profiles must lie in the wings of the primary profiles for the expected mass ratio less than four. Therefore, we expect an asymmetry, rather than a separate maximum, in the $Q(K)$ curves. To determine what degree of asymmetry would be introduced by secondaries of various intensities, artificial spectra were produced and cross-correlated. The artificial spectrum consists of a real spectrum with the addition of a secondary line profile of variable intensity inserted at the appropriate orbital phase. The line profiles used for the secondary were taken from the primary profiles of the real spectra. In order to conserve total flux removed from the continuum for any secondary amplitude, the intensity was renormalized after the addition of the secondary line profiles.

A series of artificial spectra was computed for the orbital phases corresponding to the actual spectra, assuming a mass ratio of three, as employed by Avni and Bahcall (1975) in their synthetic spectra. For a primary spectral type of O9.7 Iab (Walborn 1973), this value of the mass ratio implies that the secondary is of spectral type early B, where the He I line strengths reach a maximum. By comparing the magnitude of the asymmetry in the $Q(K)$ curve of the real spectra with those caused by secondaries of various intensities, it is possible to set an upper limit on the relative intensity of a secondary line that may be present in the real spectra.

The addition of a secondary line profile to the real spectra has the effect of broadening the primary profile. As a consequence, in addition to the expected asymmetry, there was a reduction in the peak magnitude of $Q(K)$ for the artificial spectra. This reduction in the peak magnitude of $Q(K)$ was found to obscure the comparison of symmetry between the curves for the real and artificial spectra. Since it is the symmetry of the $Q(K)$ curves which are of interest, we independently scaled the ordinate of each $Q(K)$ curve to have the same peak magnitude. This procedure only affects the vertical scale and has *no* effect on the horizontal scale (i.e., the symmetry) of the $Q(K)$ curves. The resulting $Q(K)$ curves are shown in Figures 2–4.

In order to better show any asymmetry in the $Q(K)$ curves, a dashed curve is plotted for each set which shows the right side of the $Q(K)$ curve for the real spectra, reflected about the primary peak. Comparing the left-hand side of $Q(K)$ to the reflected right-hand side makes any asymmetry readily apparent. When these two curves are very close, this closeness sets an upper bound to the asymmetry.

IV. RESULTS

The λ4026 $Q(K)$ curves (Fig. 2) are disappointing because of the apparent lack of sensitivity of the function to the presence of a luminous secondary. This lack of sensitivity can be attributed to the fact that the orbital phases of the spectra are not evenly distributed around the period. The spectra were all obtained at orbital phases where the primary (secondary) is always

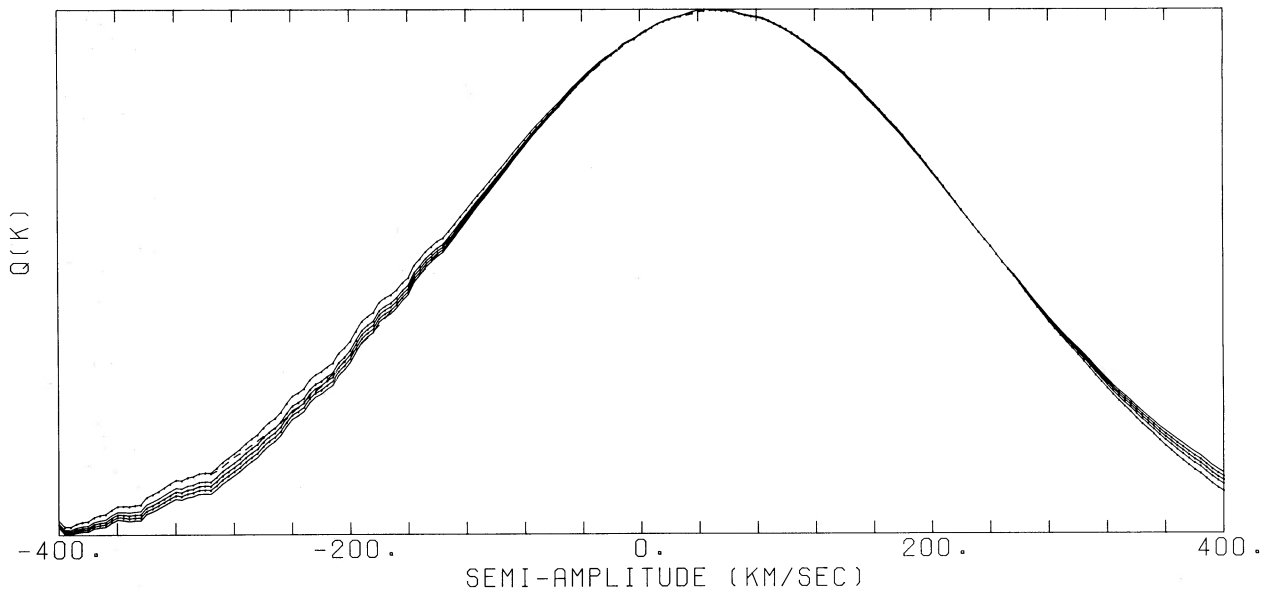

FIG. 2.—Results of the cross-correlation for the λ4026 spectra. The merit function, $Q(K)$, is plotted vs. assumed velocity amplitude, K. *Solid line:* $Q(K)$ for the raw observations; *dotted lines:* $Q(K)$ for the data with the addition of an artificial secondary star, with intensity relative to the primary of 2, 4, 6, and 10%, reading bottom to top; *broken line:* reflection of the right-hand side of the solid line about the peak K value, included to illustrate the deviation from symmetry of the merit function.

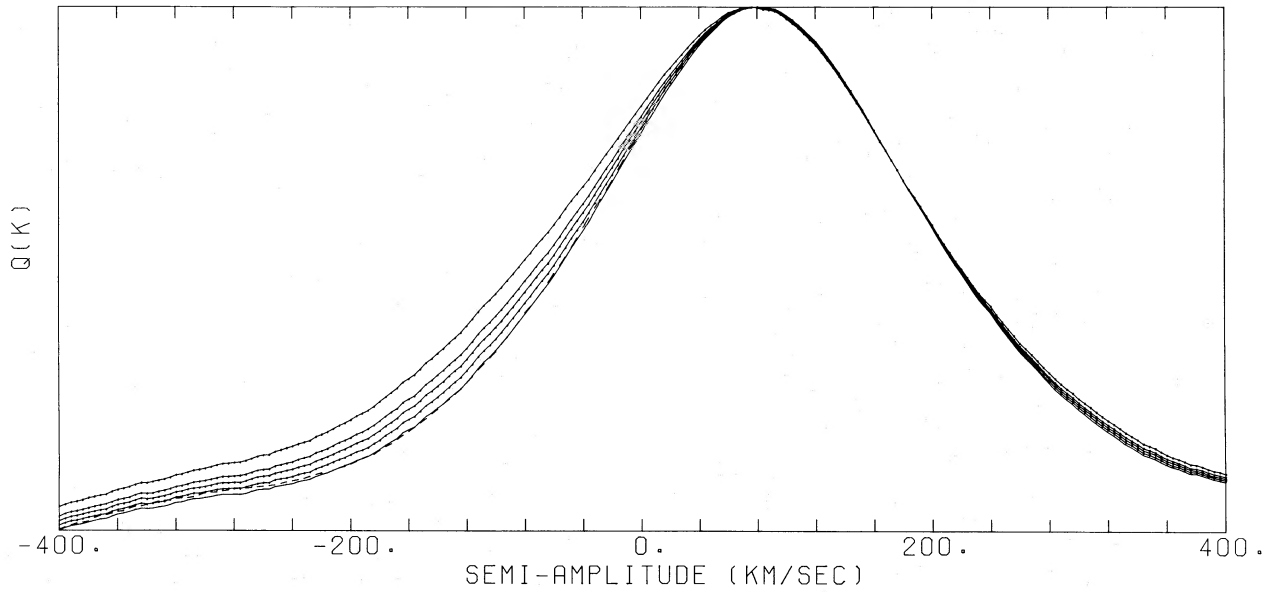

FIG. 3.—Merit function for the λ4471 spectra; the various curves are plotted with the same convention as described for Fig. 2. The strongest constraints on the presence of a luminous secondary are derived from these data.

redshifted (blueshifted). Consequently, the spectral arrays all shift in the same direction with K during the correlation process. The spectral features move slowly relative to one another, making $Q(K)$ a broadly peaked function. As a result of the broad peaks, the $Q(K)$ curves for the artificial spectra do not deviate significantly from the symmetry of the curve for the real spectra. This lack of differentiation between the $Q(K)$ curves for the real and artificial spectra reflects the insensitivity of the λ4026 data to the presence of a secondary. Although the lack of sensitivity prohibits an accurate determination of an upper limit on the relative intensity of a secondary, a conservative examination of the $Q(K)$ curves indicates an upper limit of 10%.

The results for the λ4471 data (Fig. 3) are more useful and interesting. There is a significant distinction between the $Q(K)$ curves for the real and artificial spectra as indicated in Figure 3. Referring to the dashed curve, we see that the curve for the real spectra is very nearly symmetric about the primary peak. A comparison between the curves for the real and

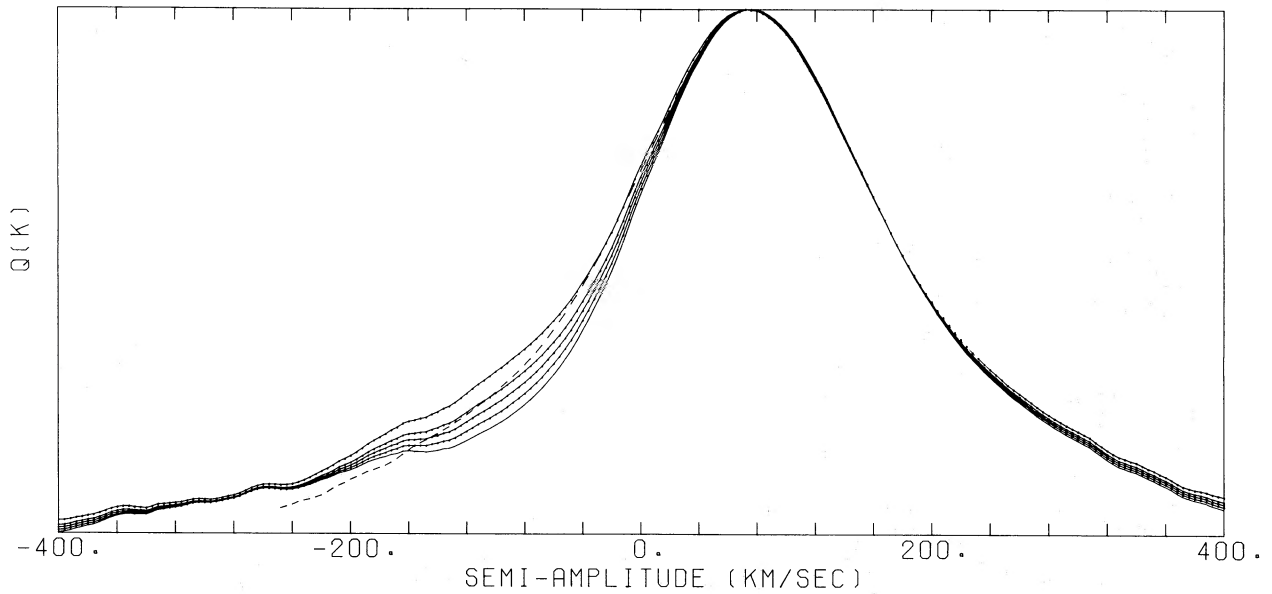

FIG. 4.—Merit function for the λ5876 spectra

artificial spectra indicates that the curve for the real spectra is symmetric within the uncertainty defined by a 2% secondary.

The $Q(K)$ curves for the λ5876 data are shown in Figure 4. The curve for the real spectra is asymmetric at the 10% secondary level; however, the asymmetry is in the opposite sense to what we expect for the effect of a luminous secondary. This "backward" asymmetry may be the result of asymmetry in the primary line profiles, either intrinsic to the star (e.g., due to a stellar wind) or because of fluctuations in the data.

On the basis of the $Q(K)$ curves for the λ4471 spectra, we argue that if a luminous secondary is present, it must have an intensity below 2% of the primary. The results for both the λ4026 and λ5876 data are consistent with this.

In principle, it should be possible to determine the semiamplitude of the primary from $Q(K)$. In practice, however, the relatively large widths of $Q(K)$ prohibit an accurate determination. On the basis of $Q(K)$ for the $\lambda\lambda$4471, 5876 spectra, we estimate the primary's K as 78 ± 10 km s^{-1}, which is consistent with Bolton's (1975*a*) value of 72.2 km s^{-1}. $Q(K)$ for the λ4026 spectra peaks at a somewhat lower value of K (~ 50 km s^{-1}); we attribute this low value to the particularly poor distribution of the individual λ4026 spectra around the orbit, resulting in the broad $Q(K)$ curve. Our result for K is not strictly independent of Bolton's value because we employ his other orbital elements in our correlation algorithm. We could simultaneously determine K, e, ω, P, and T, but our estimates of quantities other than K would be very poor because we have so few spectra.

V. CONCLUSION

Based on our examination of $Q(K)$ for all three sets of spectra, we conclude that the presence of a luminous stellar secondary is *not* indicated from our analysis of the HDE 226868 spectra. Furthermore, a conservative examination of the $Q(K)$ curves for the λ4471 data shows that a secondary with an intensity greater than 2% of the primary would have been seen. If the two stars have approximately the same spectral type, as expected because of the small mass ratio, then we have established a lower bound of 4 mag on their differance in blue light. The exact value of this bound depends on the confidence with which we are willing to assert that in Figure 3 $Q(K)$ contains no broad bulge on its wing. In turn, this depends on the confidence we have that the effects of a secondary are not canceled by a negative feature intrinsic to the primary, the data, or the analysis. For example, we have not considered the effects of tidal distortion, minor variations in the assumed mass ratio (e.g., Bolton 1975*a*), or gravity darkening of the primary, all of which could affect our limit on the relative intensity of the secondary. Finally, this confidence is derived from the smoothness, regularity, and symmetry of $Q(K)$ in the regions where a secondary could not contribute. This is a qualitative, as well as a statistical, question, and readers may judge for themselves, using our observed and synthesized $Q(K)$ as a guide. Our limit is somewhat more restrictive than Bolton's (1975*b*) bound of 3 mag, which he obtained by co-adding tracings of photographic spectra of the same orbital phase and looking directly for the secondary line profile. Like our result, his bound depends on a partially subjective judgment that a curve does not contain a secondary dip, and that accidental cancellation of such a dip by some other effect is unlikely.

Avni and Bahcall (1975) have calculated a number of possible models for the Cyg X-1 system where the secondary is a main-sequence early-B star of 9–11 $M_\odot$. They conclude that such secondaries contribute 5–13% to the blue-light curve. Furthermore, they find that this range can be expanded somewhat in the event that the secondary star is either above the main sequence (increasing the light contribution to $\sim$25%), or is a peculiar star with a radius below that of the main sequence (lowering the contribution to $\sim$2%). Our upper limit of 2% on the relative intensity of the secondary rules out all of their models which contain main-sequence stars. Indeed, even a 5% limit would rule out such models for masses greater than $\sim 9\ M_\odot$. However, a secondary below the main sequence could evade detection in our analysis. Because of the model-dependent nature of the Avni and Bahcall calculations, we cannot unequivocably rule out the existence of a luminous secondary star. However, our 2% limit makes the viability of such an alternative to the existence of a black hole in Cyg X-1 most unlikely.

We are pleased to acknowledge the continued assistance of Mr. Greg Schmidt in the detector design and development, as well as in obtaining the observations. We also thank the referee for comments and suggestions which resulted in improvement of this paper. Financial support for this work has been provided by the National Science Foundation, through grants AST 77-27745 (B. M.) and AST 78-15431 (J. I. K.), the National Aeronautics and Space Administration, through grants and contracts NGR 05-009-188 and NAS 5-24463 (R. J. H.) and NSG 7341 (J. I. K.), and the Alfred P. Sloan Foundation (B. M., J. I. K.).

REFERENCES

Abt, H. A., Hintzen, P., and Levy, S. G. 1977, *Ap. J.*, **213**, 815.
Avni, Y., and Bahcall, J. N. 1975, *Ap. J.*, **197**, 675.
Bahcall, J. N., Dyson, F. J., Katz, J. I., and Paczyński, B. 1974, *Ap. J. (Letters)*, **189**, L17.
Bahcall, J. N., Rosenbluth, M. N., and Kulsrud, R. M. 1973, *Nature Phys. Sci.*, **243**, 27.
Beaver, E. A., Harms, R. J., and Schmidt, G. M. 1976, *Adv. Electronics Electron Phys.*, **40B**, 745.

Beaver, E. A., and McIlwain, C. E. 1971, *Rev. Sci. Instr.*, **42**, 1321.
Bolton, C. T. 1972, *Nature*, **240**, 124.
———. 1975*a*, *Ap. J.*, **200**, 269.
———. 1975*b*, in *X-ray Binaries*, ed. E. Boldt and Y. Kondo, NASA SP-389, p. 465.
Fabian, A. C., Pringle, J. E., and Whelan, J. A. J. 1974, *Nature*, **247**, 351.
Hutchings, J. B. 1974, *Ap. J.*, **188**, 341.
Hutchings, J. B., Crampton, D., Glaspey, J., and Walker, G. A. H. 1973, *Ap. J.*, **182**, 549.
Shipman, H. L. 1975, *Ap. Letters*, **16**, 9.
Walborn, N. R. 1973, *Ap. J.* (*Letters*), **179**, L123.

RICHARD J. HARMS: Department of Physics, B-019, University of California, La Jolla, CA 92093

JONATHAN I. KATZ AND ALLEN W. SHAFTER: Department of Astronomy, University of California, Los Angeles, CA 90024

BRUCE MARGON: Astronomy Department, FM-20, University of Washington, Seattle, WA 98195